



Synthesis of TAT peptide-tagged PEGylated chitosan nanoparticles for siRNA delivery targeting neurodegenerative diseases

Meenakshi Malhotra, Catherine Tomaro-Duchesneau, Satya Prakash*

Biomedical Technology and Cell Therapy Research Laboratory, Department of Biomedical Engineering, Artificial Cells and Organs Research Center, Faculty of Medicine, McGill University, 3775 University Street, Montreal, Quebec H3A 2B4, Canada

ARTICLE INFO

Article history:

Received 25 August 2012

Accepted 4 October 2012

Available online 8 November 2012

Keywords:

Chitosan

PEG

TAT

siRNA

Nanoparticles

Gene delivery

ABSTRACT

Delivery of therapeutic molecules to the brain for the treatment of Neurodegenerative diseases (ND) is a challenging task. This manuscript introduces a novel scheme of synthesizing peptide-tagged polyethylene glycol (PEG)ylated chitosan polymer to develop nanoparticles for siRNA delivery for use in ND. Specifically, this manuscript proposes a facile chemoselective conjugation of monomethoxy PEG, at the C2 hydroxyl group of chitosan polymer, with conjugation of PEG to a cell-penetrating peptide, Trans-Activator of Transcription. The synthesized Chitosan-PEG-TAT polymer was used to form the nanoparticles of approximately 5 nm, complexing siRNA to be delivered in neuronal cells (Neuro 2a), with no/minimal toxicity. The various intermediates and the final product formed during the synthesis were characterized using ¹H Nuclear Magnetic Resonance and Fourier Transform Infrared Spectroscopy spectra. The morphological details of the nanoparticles were studied using Transmission Electron Microscopy. The nanoparticles were tested to deliver a functional siRNA against the Ataxin-1 gene in an in-vitro established model of a ND Spinocerebellar ataxia (SCA1) over-expressing ataxin protein. The results indicate successful suppression of the SCA1 protein following 48 h of transfection. Result of this study has potential in ND like SCA, Parkinson's, Alzheimer's and others.

Crown Copyright © 2012 Published by Elsevier Ltd. All rights reserved.

1. Introduction

Neurodegeneration is characterized by the progressive loss of structure and function of neurons. One among many neurodegenerative diseases is Spino Cerebellar Ataxia (SCA), characterized by a loss of cells of the cerebellum and spinal cord affecting motor coordination, posture and balance. The international prevalence of SCA is estimated to be 0.3–2.0 per 100,000 [1]. SCA is caused by polyglutamine trinucleotide repeat expansion, CAG repeat and forms an abnormal/mutant protein when the CAG repeat unit is above the threshold level, i.e. approximately 35 repeat units [2]. The abnormal protein then accumulates in the Purkinje cells of the brain and also cytoplasm, dendrites and axonal processes [2]. A recent review by our group highlights the different subtypes of SCA and the current therapeutic methods and drugs used to alleviate the symptoms of this disease [2]. The reason for the absence of available medication could be attributed to the genetic problem associated with it. In the case of SCA, the cell production of poly

glutamine cannot be halted as it would interfere with the function of the brain cells and, thus, would produce side-effects which may in turn require further treatment. However, certain drugs like Deferipone and Idebenone [3] have reached phase II and III clinical trials, respectively, but are limited to Friedreich's ataxia (Autosomal Recessive Cerebellar Ataxia). Several other reports on the active and completed clinical trials of other related neurodegenerative diseases can also be found at clinicaltrials.gov.

RNA interference technology has been demonstrated as an effective therapeutic modality *in vivo* for the reduction of pathological molecules in neurons, for the treatment of Spinocerebellar Ataxia [4]. The other therapeutic targets that have been successfully inhibited with siRNA include ion channels [5], growth factors [6] growth factor receptors [7] and transcription factors [8]. The currently used drug/therapeutic delivery strategies such as implantation of catheters, intra-carotid infusions, surgeries and chemotherapies are invasive in nature and pose a greater risk of post-surgical complications like fluid retention in the ventricles etc, which lead to fatal side-effects. It has been estimated that up to 98% of the newly developed small molecules do not cross the blood–brain barrier [9]. Moreover, it is challenging to achieve sufficient distribution and diffusion of the therapeutic drug within the brain. Although viral gene therapy vectors are the most efficient vectors

* Corresponding author. 3775 University Street, Room 311, Department of Biomedical Engineering, Lyman Duff Medical Building, Montreal, Quebec H3A 2B4, Canada. Tel.: +1 514 398 2736; fax: +1 514 398 7461.

E-mail address: satya.prakash@mcgill.ca (S. Prakash).

available [4] concerns about their safety and immunogenicity [10] have triggered investigations of non-viral delivery systems. Thus, a need to develop an alternative non-invasive and targeted therapeutic delivery strategy exists which can cross/bypass the blood–brain barrier.

The current research focuses on developing a scheme to synthesize non-viral, receptor-targeted nanoparticle formulation for the delivery of siRNA molecules capable of targeting neuronal cells. The scheme utilizes and preserves the unique characteristic of each component (Chitosan, PEG and a cell-penetrating peptide). Chitosan is a polycationic polymer that has been regarded as a non-toxic [11], biodegradable [12] and biocompatible [13] polysaccharide. Due to the presence of primary amine groups, it is only soluble in dilute acids. The presence of free amine groups helps in complexing the negatively charged therapeutic molecules simply by ionic interactions. The free amine groups also help in cellular uptake of chitosan-derived nanoparticles, leading to a “proton sponge effect” in the endosomal compartment. The cationic biodegradable polymers are usually surface coated with hydrophilic polymers like polyethylene glycol (PEG). PEG has been extensively used in biomedical and pharmaceutical applications because it is hydrophilic, non-toxic, non-antigenic and non-immunogenic [14]. PEG, helps eliminate phagocyte capture, providing better serum stability and extended blood circulation with low toxicity.

Many studies have conjugated PEG with amine groups of chitosan in view of improving its solubility in both aqueous as well as organic solvents [15,16]. The most extensively used is α -Methoxy, ω -hydroxy PEG (MeO-PEG). The use of a monofunctional PEG is important to avoid crosslinking reactions between the two polymers [17]. Whereas, a bifunctional PEG serves as a linker for conjugating two different compounds, being neutral in charge, it reduces the steric-hindrance of the charged polymers and thus enables the efficient conjugation of two compounds linked on either side. However, PEG increases the blood clearance times of the nanoparticles but at the same time compromises its transfection efficiency, as PEG masks the overall charge on the surface of chitosan polymer. Therefore, a cationic cell targeting/penetrating peptide is required to interact with the negatively charged cell surface proteoglycans [18]. The transfection efficiency of many other delivery vehicles apart from chitosan have been shown to improve with the incorporation of functional groups, such as targeting ligands or Nuclear localization signal (NLS) peptides [19].

This paper proposes a step-wise protocol for synthesizing peptide-tagged PEGylated chitosan, wherein PEG acts as a linker between chitosan and a cell-penetrating peptide. We have employed the use of TAT oligopeptide, as a model cell-penetrating peptide, covalently conjugated to the chitosan-PEG copolymer. The basic domain of TAT peptide (RKKRRQRRR) is comprised of arginine and lysine amino acid residues that can play an important role in the translocation across biological membrane due to its strong cell-adherence and is independent of receptors and temperature [20]. TAT has been shown to destabilize the lipid bilayer of the cell membrane through an energy independent pathway carrying hydrophilic or macromolecules as large as several hundred nanometers in size across the plasma membrane [21]. The current study shows the efficiency of TAT peptide-tagged PEGylated chitosan nanoparticles formed after step-wise chemo-selective synthesis process, to deliver siRNA in neuronal cells and cause a therapeutic effect by suppressing the Ataxin-1 protein.

2. Materials and methods

Low Molecular weight (LMW) chitosan was obtained from Wako (Richmond, VA, USA), having a viscosity of 5–20 cP and degree of deacetylation of 80.0%. Polyethylene glycol monomethyl ether (mPEG) (M.W. 2000), phthalic anhydride, pyridine, toluene,

hydrazine monohydrate, succinic anhydride, ethanethiol, aluminum chloride, sodium tripolyphosphate (TPP) and glacial acetic acid of analytical grade were obtained from Sigma (Oakville, ON, Canada). Anhydrous N,N-Dimethylformamide (DMF), 1-ethyl-3-[3-dimethylaminopropyl]carbodiimide hydrochloride (EDC), 4-(Dimethylamino)pyridine (DMAP), sodium hydroxide (NaOH), methanol, diethyl ether, chloroform and concentrated hydrochloric acid were obtained from Thermo Fisher Scientific (Ottawa, ON, Canada). Thionyl chloride (SOCl₂) was obtained from VWR (Mississauga, ON, Canada). TAT peptide (NH₂-RKKRRQRRR) M.W. 1339.63 was synthesized by the Sheldon Biotechnology Centre, McGill University. Mouse Neuro2a cells and EMEM media were obtained from Cedarlane laboratories (Burlington, Ontario, Canada). MTS cytotoxicity assay kit was obtained from Promega (Madison, WI, USA). Subcloning DH5- α competent cells and Lipofectamine 2000 were obtained from Invitrogen (Burlington, ON, Canada). pEGFP.ataxin1 (E3-82Q) plasmid is obtained from Dr. Zoghbi Huda from Baylor College of Medicine, Houston, TX, USA. Plasmid purification Maxi kit is from Qiagen (Mississauga, Ontario, Canada). Ataxin-1 siRNA (h), Ataxin-1(L-19) goat polyclonal antibody, Actin (I-19) goat polyclonal antibody and (HRP)-conjugated donkey anti-goat IgG antibody were procured from Santacruz Biotechnology (Santa Cruz, CA, USA). For dilution purposes ultra pure double distilled water (ddH₂O) was used from laboratory installed Barnstead Nanopure diamond™ water supply unit.

2.1. Synthesis of CSPH (phthaloyl chitosan)

Commercially available chitosan (CS) (1.00 g) was added to a solution of phthalic anhydride (PH) (2.76 g) in 20 ml of N,N-Dimethylformamide (DMF). The mixture was stirred for 8 h at 110 °C under nitrogen atmosphere. The resultant product (c) in Fig. 1 was cooled to room temperature and precipitated in ice cold water [22]. The precipitate was filtered, washed with methanol overnight and vacuum dried.

2.2. Synthesis of mPEG-COCl

To 10% solution of mPEG (M.W. 2000) in toluene, 4 M excess of succinic anhydride dissolved in pyridine was added drop-wise. The above reaction was set up under anhydrous conditions and refluxed for 6 h. The product was precipitated with ether, filtered and again re-precipitated twice with chloroform and diethyl ether and finally vacuum dried. The final product obtained (a), is shown in Fig. 1. To mPEG-COOH obtained, 2 fold molar excess of SOCl₂ was added under N₂ atmosphere. The reaction was refluxed to boil for 6 h, followed by degassing to remove excess SO₂ and thionyl chloride. The product was marked as (b) in Fig. 1.

2.3. Synthesis of CSPH-O-mPEG (PEGylating phthaloyl chitosan)

Phthaloyl chitosan (CSPH) (300 mg), product (c), was soaked in pyridine solution overnight and added to mPEG acylchloride (10 g), product (b), in toluene. The reaction was stirred for 2 h at room temperature and then refluxed to boil for 24 h [23]. The resultant product was allowed to cool to room temperature, precipitated in methanol and vacuum dried to yield product (d) in Fig. 1.

2.4. Synthesis of CSPH-PEG-TAT (Tagging TAT on PEGylated phthaloyl chitosan)

To conjugate TAT peptide onto PEGylated phthaloyl chitosan, the methoxy group of PEG was converted to hydroxyl group by following the procedure, as aforementioned [24]. In brief equi-molar ratios of CS-mPEG and aluminum chloride were reacted together for 12 h at room temperature (RT) in 20 ml of ethanethiol. The reaction mix was diluted with water, acidified with 10% HCl, filtered and extracted thrice with dichloromethane to yield product (e) in Fig. 1. The hydroxyl groups were further converted to carboxyl groups by reacting it with 4 M excess of succinic anhydride in toluene at 100 °C for 12 h. The product obtained as (f) in Fig. 1 was cooled to room temperature, precipitated with methanol, filtered and vacuum dried. The carboxylic groups of this product (f) i.e. CS-PEG-COOH (12 mM) was conjugated to the equi-molar ratio of TAT-NH₂ peptide (12 mM) in the presence of EDC (15.5 mM) and DMAP (1.2 mM) in 1 ml of DMF at RT for 24 h. This reaction mix was dialyzed against deionized water for 2 days, using a dialysis tube with a molecular weight cut-off of 3500 Da. The resultant product (g) was obtained as shown in Fig. 1.

2.5. Synthesis of CS-PEG-TAT (deprotecting amine groups on chitosan)

As a last step of the synthesis, the amine groups of chitosan were deprotected using 4% (w/v) hydrazine monohydrate in DMF. The reaction was carried out at 100 °C for 1 h under inert conditions. The mixture was allowed to cool to room temperature and was dialyzed against deionized water for 2 days, using a dialysis tube with molecular weight cut-off of 3500 Da. Following dialysis, the sample was vacuum dried and marked as product (h) in Fig. 1.

2.6. Polymer characterization

The polymer CS-PEG-TAT was characterized and analyzed at every step of its derivation through FTIR (Perkin Elmer Spectrum BX), ¹³C NMR (Varian 300 MHz

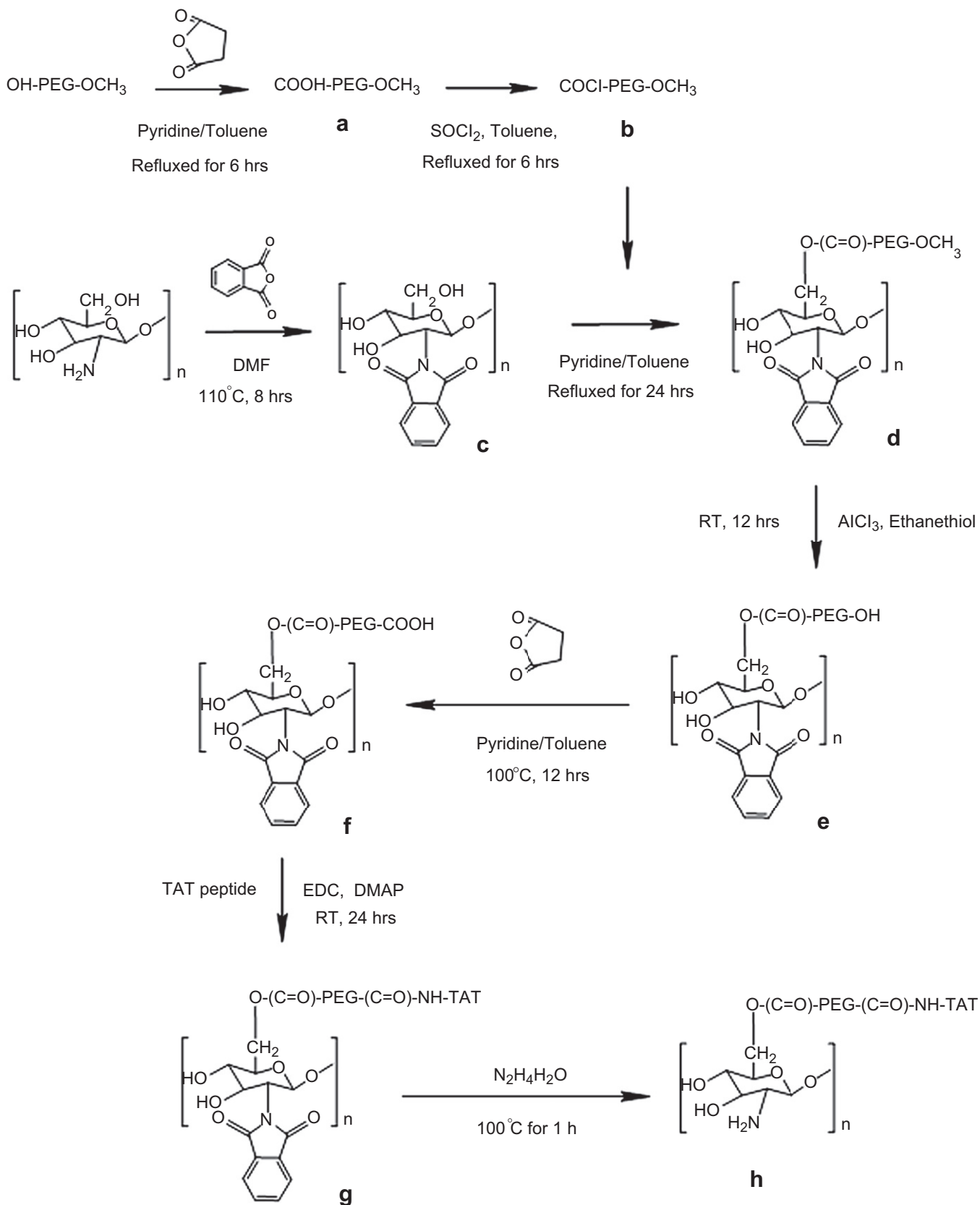


Fig. 1. Chemoselective synthesis of chitosan polymer: Schematic representing the synthesis route of peptide-tagged PEGylated chitosan polymer for the development of receptor-targeted nanoparticles.

broadband NMR) and ^1H NMR (Mercury 400 and 500 MHz NMR) and Transmission Electron Microscopy (Philips EM410 TEM).

2.7. Preparation of siRNA complexed CS-PEG-TAT nanoparticles

The obtained CS-PEG-TAT polymer was dissolved in ddH₂O at pH 5.0, and concentration of 0.5 mg/ml. To ensure maximum dissolution of the polymer, the solution was heated at 60 °C and sonicated followed by stirring for 60 min. Before nanoparticle formation the polymer solution was filtered using 0.8 μm filter. The nanoparticles were prepared by mixing 2 μg of siRNA (calculated per ml of polymer solution), in 200 μl of 0.7 mg/ml sodium tripolyphosphate (TPP), pH 3. The siRNA-TPP solution was then added drop-wise to 800 μl of polymer solution and kept at continuous stirring for 1 h at 800 rpm. The nanoparticles obtained were viewed under TEM.

2.8. Plasmid purification – ataxin-1 cDNA

The plasmid DNA containing ataxin-1 cDNA, purified and resuspended in Tris-EDTA buffered solution [pGFP-ataxin (Q82)] was a kind gift from Dr. Zoghbi Huda (Baylor college of medicine, Houston, TX, USA), and was used for the transformation experiment in DH5- α competent cells by means of chemical transformation also known as Heat shock transformation. The procedure for chemical transformation was followed according to the manufacturer's protocol (Invitrogen). The colony selective antibiotic for pGFP-ataxin was kanamycin (30 $\mu\text{g}/\text{ml}$). Stock cultures of transformed plasmid in DH5- α cells were made in sterilized 80% glycerol and were stored at -80 °C. Plasmid purification was performed following the protocol of Qiagen's maxi kit. The purified plasmid obtained was quantified for its concentration and purity. The percentage purity of the plasmid was quantified using UV spectrophotometer. The ratio of Abs 260/280 obtained was 1.8 which signifies that the plasmid was purified and the concentration obtained was 266 $\mu\text{g}/\text{ml}$ for pEGFP.ataxin1.

2.9. Cell study

Cell study with respect to transfection efficiency of the nanoparticles encapsulating siGLO-red (Cy5-labeled transfection indicator) and cellular toxicity of nanoparticles using MTS assay was performed on mouse neuroblastoma cells (Neuro 2a).

2.9.1. Transfection efficiency of siRNA loaded nanoparticles on Neuro2a cells

The transfection studies were performed on mouse neuroblastoma cells (Neuro2a). The cells were allowed to reach 85% confluency sub-culture and seeding in a 96 well plate at a density of 20,000 cells per well. Twenty four hours before transfection, cell seeding was carried out with 200 μl of complete growth media (antibiotics-free EMEM with 10% serum) in each well. Following 24 h, the transfection media containing 100 μl of serum-free medium along with 50 μl of sample was added onto the cells. The different tested samples were: chitosan nanoparticles encapsulating siGLO-red and chitosan-PEG-TAT nanoparticles encapsulating siGLO-red. The cells were then incubated at 37 °C, 5% CO₂ for 4 h, after which the cells were replaced with fresh complete media (with FBS). After 24 h, the cells were observed under a fluorescence microscope (Nikon Eclipse TE2000-U) at a wavelength of 660 nm. The property of siGLO-red as a transfection indicator gene, allows it to fluoresce inside the cell, enabling them to be viewed under a fluorescent microscope.

2.9.2. Cytotoxicity analysis

The cytotoxicity assay was performed on seeded cells following 4 h of transfection in 96 well plate. The transfection media was removed following 4 h and the cells were replenished with 100 μl of fresh serum-free media, to which 20 μl of MTS reagent was added and the cells were again incubated for another 4 h at 37 °C in 5% CO₂ incubator. The absorbance was measured using Varian multiplate reader set at 490 nm.

2.9.3. Over-expression of ataxin protein in Neuro2a cells and its suppression

Transfection studies were performed using a functional siRNA against the ataxin gene. 100,000 cells were seeded in a 12 well plate and were incubated for adherence for 24 h at 37 °C, 5% CO₂. After 24 h, the cells were transfected with ataxin plasmid at a concentration of 250 ng/ μl using lipofectamine. Optimal transfection efficiency with lipofectamine was determined experimentally. Following 6 h of transfection, the media was replaced with complete growth EMEM medium containing 10% FBS. Ataxin-siRNA (SantaCruz Biotechnology) was complexed with chitosan-PEG-TAT nanoparticles, as described in Section 2.7. After 24 h, 40 μm per well of siRNA complexed with nanoparticles was used to transfect neuronal cells. Again, the transfection media was replaced with complete growth EMEM medium containing 10% FBS. Empty nanoparticles and nanoparticles containing scrambled siRNA were used as positive controls. The cells were harvested for ataxin protein estimation after 24 and 48 h.

2.10. Protein extraction and western blot

Cultured cells were washed twice with cold PBS and lysed using 1% NP40 prepared in 50 mM Tris (pH 8.0), 150 mM NaCl, 5 mM EDTA lysis buffer; premixed with

2 \times SDS sample buffer (125 mM Tris HCl, pH 6.8; 4% SDS; 20% glycerol; 100 mM DTT, and 0.2% bromophenol blue) at 4 °C on an orbital shaker. The cells were scraped after 20 min (on ice). The extracted protein samples were heated at 70–100 °C for 10 min, before loading on gels. The western blot was performed according to manufacturer's protocol (Invitrogen). Pre-cast Nupage Tris-Bis (4–10%) gels were used for running the protein samples. Magic mark 1 Kb protein ladder was used as a standard. The gel was electrophoretically transferred to a nitrocellulose membrane using SemiDry blot apparatus (Invitrogen). The membrane was incubated for 1 h in 5% non-fat powdered milk in 0.2% TBST. The membrane was then incubated overnight with goat ataxin-1 IgG polyclonal antibody (1:5000 dilution; SantaCruz Biotechnology). After three washes in TBST, the membrane was incubated with horseradish peroxidase (HRP)-conjugated donkey anti-goat IgG antibody (1:2000 dilution; SantaCruz Biotechnology). The membranes were then washed three times in TBST followed by detection of signal with a chemiluminescence detection kit (Roche). To control the protein loading, the membrane was stripped at 60 °C using stripping solution (10 mM β -mercaptoethanol, 2% SDS, and 62.5 mM Tris-HCl, pH 6.8) before reprobing with antibody to α -Actin (1:10,000; Santa Cruz Biotechnology).

2.11. Statistical analysis

Values are expressed as means \pm Standard Deviation. Statistical analysis was carried out using SPSS Version 17.0 (Statistical Product and Service Solutions, IBM Corporation, New York, NY, USA). Statistical comparisons were carried out by using the general linear model (GLM) and Tukey's post-hoc analysis. Statistical significance was set at $p < 0.05$ and p -values less than 0.01 were considered highly significant.

3. Results

3.1. Synthesis of CSPH (phthaloyl chitosan)

The commercially available chitosan polymer with degree of deacetylation (DA) of 80% was first protected with phthalic anhydride in order to protect the amine groups. This is the key step in carrying forward any further chemical reactions with chitosan, as chitosan being soluble only in acidic conditions becomes soluble in most organic solvents such as DMSO, DMF, THF, Pyridine etc. following protection with phthalic anhydride. ^{13}C NMR data confirms successful N-phthaloylation of the product. Product (c) in Fig. 1 shows the schematic representation of the N-phthaloyl chitosan. The Total Suppression of Side bands (TOSS) mode exhibit peaks at 124.62 ppm, 131.70 ppm, 134.42 ppm corresponding to phenylene, and 169.66 ppm and carbonyl group of phthaloyl group and the TOSS and dipolar dephasing (TOSDL) mode confirms the absence of CH and CH₂ peaks due to their short relaxation time and presence of only two peaks 131.63 ppm and 169.89 ppm assigned to C 1, 2 and carbonyl of phthaloyl group respectively. The infrared (IR) data shows distinct sharp peaks at 1774 cm^{-1} and 1702 cm^{-1} corresponding to the imide of phthaloyl group in Fig. 2. The phthaloyl chitosan prepared by this method becomes gel-like when precipitated in water, which supports the data shown by kurita, of formation of a uniform structure of phthaloylated chitosan [22].

^{13}C CP/MAS NMR: (TOSS mode): δC 58.19 (C-2), 61.76 (C-6), 72.44 (C-3), 75.42 (C-5), 83.91 (C-4), 101.24 (C-1), 124.62, 131.70, 134.42 (Phth phenylene), and 169.66 (Phth C=O); (TOSDL mode): δC 131.63 (Phth C-1,2) and 169.89 (Phth C=O).

FTIR: $\nu_{\text{max}}/\text{cm}^{-1}$ 3200–3400 (OH), 1774, 1710 (carbonyl anhydride), 1150–1000 (pyranose), and 720 (arom).

3.2. Synthesis of mPEG-COCl

The monomethoxy PEG (OH-PEG-OCH₃) (M.W. 2000) was converted to carboxylate-terminated PEG (COOH-PEG-OCH₃) by reacting monomethoxy PEG with 4 M excess of succinic anhydride. Fig. 3 represents the IR spectra that shows the presence of carboxylic peak at 1732 cm^{-1} , confirming the presence of (–C=O) carbonyl groups on PEG. This product was further reacted with thionyl chloride to form PEG acyl chloride (COCl-PEG-OCH₃) (product b in Fig. 1) as an active intermediate of PEG to be further

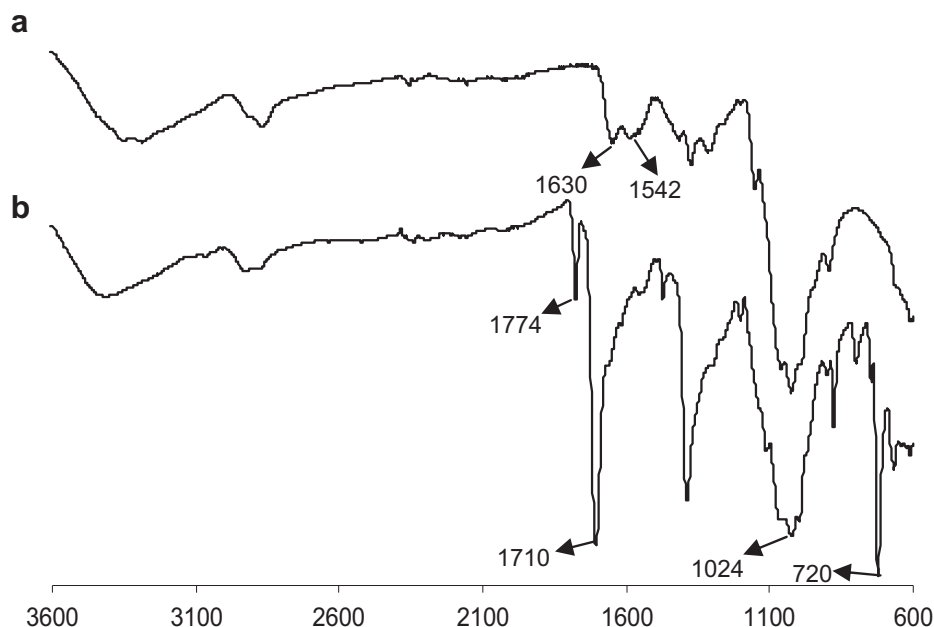


Fig. 2. Polymer characterization using FTIR: (a) commercially available chitosan (CS) and (b) 2-N-phthaloylated chitosan: $\nu_{\max}/\text{cm}^{-1}$ 3200–3400 (OH), 1774, 1710 (carbonyl anhydride), 1150–1000 (pyranose), and 720 (arom). The appearance of peak 1774 and 1710 in (b) indicate the presence of phthaloyl group on chitosan.

conjugated to hydroxyls of 2-N-phthaloyl chitosan (Product c in Fig. 1).

FTIR: $\nu_{\max}/\text{cm}^{-1}$ 1732 (C=O), 2878 (C–H stretching), 1100 (C–O stretching).

3.3. Synthesis of CSPH-O-mPEG (PEGylating phthaloyl chitosan)

The FTIR spectra in Fig. 4 shows PEG grafted phthaloylated chitosan with characteristic peaks at 2921 cm^{-1} (C–H stretching), 1066 cm^{-1} (C–O stretching), 1491, 1451 and 1254 cm^{-1} belong to PEG. Also the reduction in hydroxyl peaks of chitosan at 3500 cm^{-1} , indicates the grafting of PEG onto chitosan forming 2-N-phthaloyl chitosan-O-MPEG, product (d) in Fig. 1.

FTIR: $\nu_{\max}/\text{cm}^{-1}$ 2873 (C–H stretching), 1068 (C–O stretching) of PEG, 1774, 1710 (carbonyl anhydride) and 720 (arom) of phthalimido group on chitosan.

3.4. Synthesis of CSPH-PEG-TAT (Tagging TAT on PEGylated phthaloyl chitosan)

To attach a ligand or a cell-penetrating peptide, $\text{NH}_2\text{-TAT}$ on PEG, demethylation was performed on 2-N-phthaloyl chitosan-O-MPEG to obtain 2-N-phthaloyl chitosan-O-PEG, product (e) as shown in Fig. 1. This was performed by following steps as mentioned previously by Lin et al. [24]. This step was performed in order to obtain a reactive form of PEG that facilitates the further conjugation of

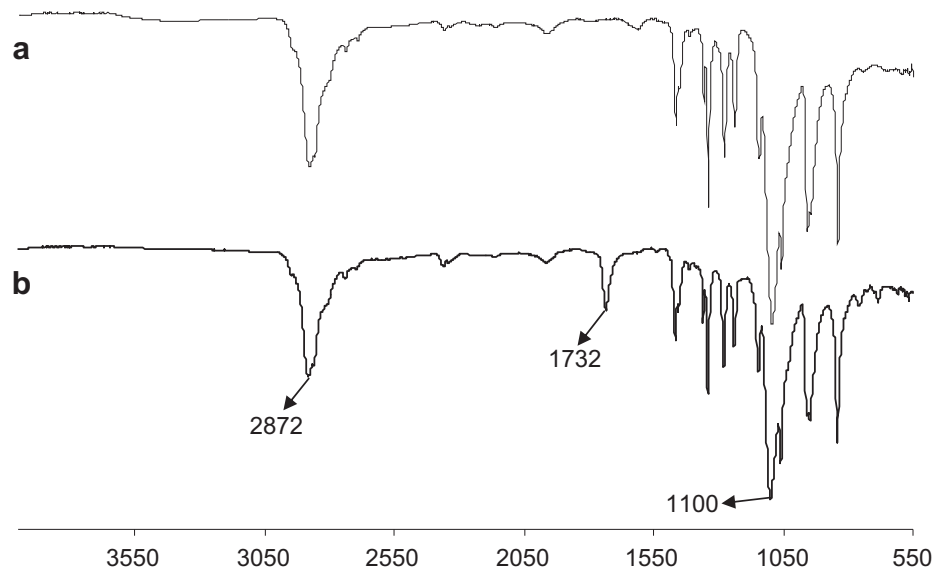


Fig. 3. Polymer characterization using FTIR: (a) Polyethylene glycol monomethyl ether (mPEG–OH) and (b) Carboxylated mPEG (mPEG–COOH): $\nu_{\max}/\text{cm}^{-1}$ 1732 (C=O), 2878 (C–H stretching), 1100 (C–O stretching). The appearance of peak 1732 in (b), indicate the successful modification of hydroxyl group to carboxyl group on PEG.

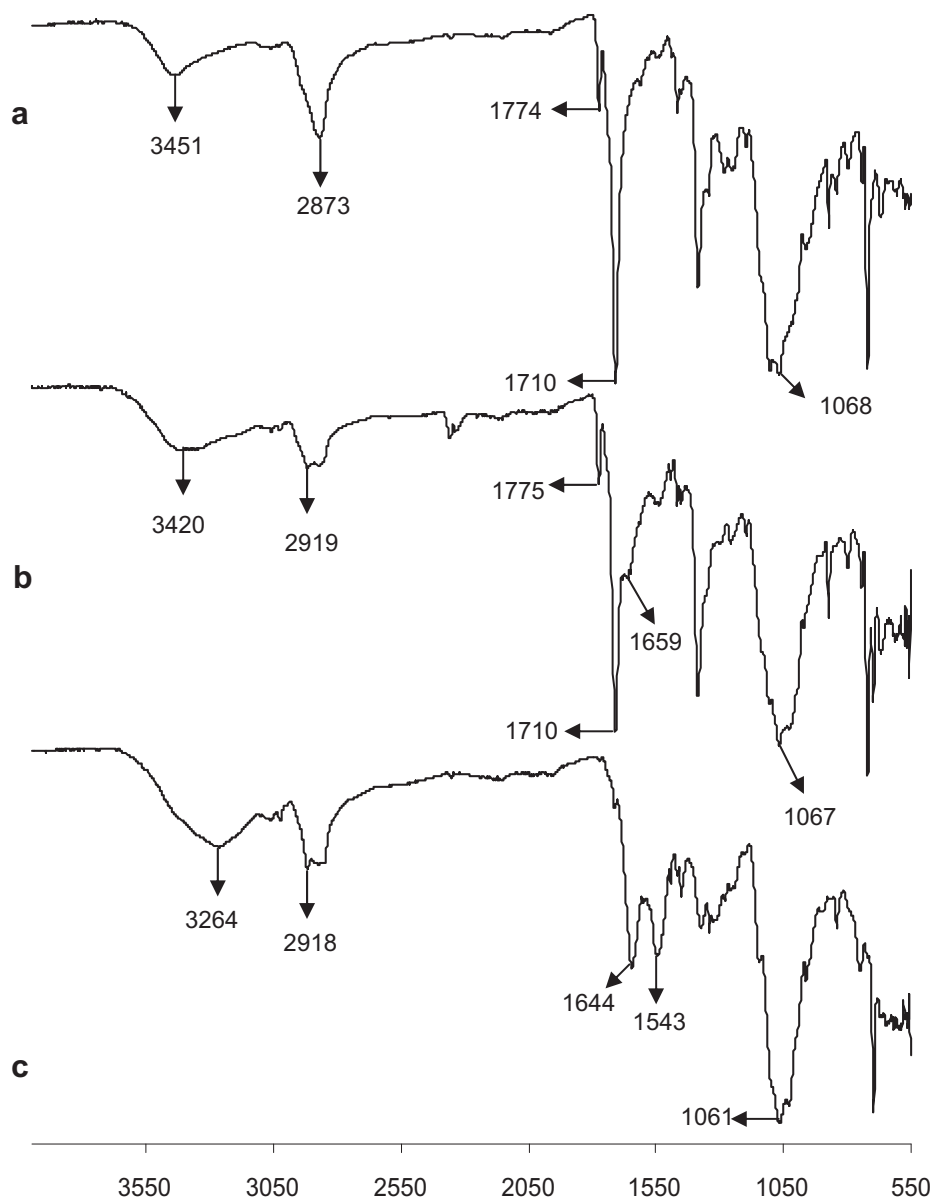


Fig. 4. Polymer characterization using FTIR: (a) 2-N-phthaloyl chitosan-O-PEG: $\nu_{\max}/\text{cm}^{-1}$ 2873 (C–H stretching), 1068 (C–O stretching) of PEG, 1774, 1710 (carbonyl anhydride) and 720 (arom) of phthalimido group on chitosan. (b) TAT tagged PEGylated phthaloyl chitosan (2-N-phthaloyl chitosan-O-PEG-CONH-TAT): $\nu_{\max}/\text{cm}^{-1}$ 2919 (C–H stretching), 1067 (C–O stretching) of PEG, 1774, 1710 (carbonyl anhydride) and 720 (arom) of phthalimido group on chitosan, 1659 (amides) in TAT peptide. (c) Deprotected TAT tagged PEGylated chitosan (chitosan-O-PEG-CONH-TAT): $\nu_{\max}/\text{cm}^{-1}$ 2918 (C–H stretching), 1061 (C–O stretching) of PEG, 1644 amides of TAT peptide, and 1543 (amides) in chitosan. The presence of peak 1659 in (b) in comparison to (a), indicate the conjugation of TAT peptide onto the polymer, as this peak shows the presence of amides that belong to TAT peptide. The absence of peak 1775 and 1740 in (c), as compared to (a and b) indicate the complete removal of phthaloyl (protecting) group from the polymer and the emergence of peak 1644 and 1543 belong to the peaks of TAT and chitosan respectively.

compounds. The product (e) was further reacted with 4 M excess of succinic anhydride under similar conditions as before. The formation of the carboxyl group at the other end of the PEG conjugated to phthaloyl chitosan enables the attachment of amine terminated TAT peptide to yield product (f) as show in Fig. 1. The IR spectra in Fig. 4 shows the appearance of a new peak at 1636 cm^{-1} that shows the presence of amide bonds and confirms the conjugation of TAT peptide onto the polymer forming 2-N-phthaloyl chitosan-O-PEG-CONH-TAT, product (g) in Fig. 1.

FTIR: $\nu_{\max}/\text{cm}^{-1}$ 2919 (C–H stretching), 1067 (C–O stretching) of PEG, 1774, 1710 (carbonyl anhydride) and 720 (arom) of phthalimido group on chitosan, 1659 (amides) in TAT peptide.

3.5. Synthesis of CS-PEG-TAT (deprotecting amine groups on chitosan)

The final step following TAT tagging was the deprotection of the amine groups from chitosan. This was successfully achieved by treating the 2-N-phthaloyl chitosan-O-PEG-CONH-TAT with 4% hydrazine monohydrate solution in DMF. Hydrazine monohydrate being basic in nature causes the destabilization of the phthaloyl moiety by creating an excess alkaline condition of $\text{pH} > 12$. The resultant product (h) as represented in Fig. 1 was obtained. The removal of the phthaloyl group from the polymer was confirmed by FTIR, where the absence of peaks at 1774 cm^{-1} and 1710 cm^{-1}

confirmed the complete dissociation of the phthalimido group from chitosan. It was observed that the reaction conditions followed in the scheme had no deleterious effects on any of the previous bonds formed. The peak representing the presence of amides due to TAT peptide shifts from 1659 cm^{-1} – 1644 cm^{-1} and the peak at 1582 cm^{-1} (amide II) belongs to the chitosan. The peaks at 2918 cm^{-1} and 1061 cm^{-1} refer to the presence of (CH_2) groups and $(\text{C}-\text{O})$ stretch) of PEG respectively as observed in Fig. 4. The final product was dialyzed for 2 days against deionized water in order to get rid of any impurity or byproduct left from the reaction.

FTIR: $\nu_{\text{max}}/\text{cm}^{-1}$ 2918 (C–H stretching), 1061 (C–O stretching) of PEG, 1644 amides of TAT peptide, and 1543 (amides) in chitosan.

3.6. Polymer characterization by ^1H NMR

Fig. 5 represents the ^1H NMR spectra of 2-*N*-phthaloyl chitosan (Fig. 5a), 2-*N*-phthaloyl chitosan-*O*-mPEG (Fig. 5b), 2-*N*-phthaloyl chitosan-*O*-PEG-*CONH*-TAT (Fig. 5c) and chitosan-*O*-PEG-*CONH*-TAT (Fig. 5d). The chemical shift at δ 7.78 belongs to the aromatic protons of the phthaloyl moiety, which is present in the spectra of 2-*N*-Phthaloyl chitosan-*O*-mPEG, 2-*N*-phthaloyl chitosan-*O*-PEG-

TAT but disappeared in chitosan-*O*-PEG-*CONH*-TAT spectrum. The multiple peaks of oxymethyl groups in PEG at δ 3.3–3.7 cover the signals of the pyranose ring of chitosan in all three spectra. The weak and broad peak at δ 4.3–4.5 were from the protons of $-\text{NH}-\text{CH}(\text{CH}_2)-\text{CO}-$ in the TAT peptide, as observed in the spectrum of 2-*N*-phthaloyl chitosan-*O*-PEG-*CONH*-TAT. The peak at δ 2.7–2.8 is from the protons of $-\text{CH}_2-\text{NH}-\text{NH}-\text{NH}_2$ in arginine and the weak and multiple peaks at δ 1.3–1.7 are from the $-\text{CH}_2-\text{CH}_2-\text{CH}_2-\text{NH}-\text{NH}-\text{NH}_2$ in arginine as observed in spectra 2-*N*-phthaloyl chitosan-*O*-PEG-*CONH*-TAT and chitosan-*O*-PEG-*CONH*-TAT. The multiple peaks at δ 7.0–8.0 belong to the amines in the TAT peptide sequence (Fig. 5e).

3.7. Preparation of siRNA complexed CS-PEG-TAT nanoparticles

Fig. 6 represents TEM images of the polymer chitosan-*O*-PEG-*CONH*-peptide dissolved in dilute acetic acid at pH 6 and a concentration of 0.5 mg/ml, sonicated for 10 min before being observed under the TEM. Fig. 6a shows nanoparticles formed with the modified Chitosan-PEG-peptide polymer, without siRNA, using TPP as a crosslinker. The nanoparticles range in the size of 50–100 nm. Fig. 6

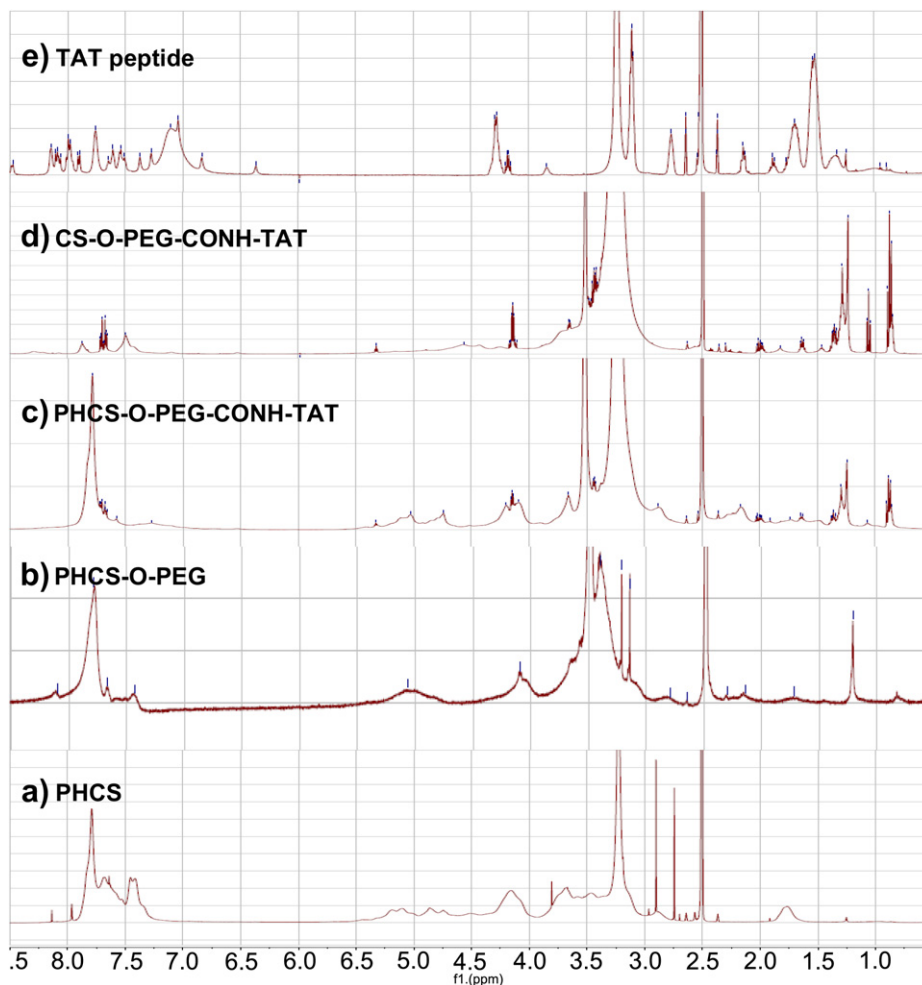


Fig. 5. Polymer characterization using ^1H NMR: (a) phthaloylated chitosan (PHCS), (b) PEGylated phthaloyl chitosan (PHCS-*O*-PEG), (c) TAT tagged PEGylated phthaloyl chitosan (PHCS-*O*-PEG-*CONH*-TAT), (d) Deprotected TAT tagged PEGylated chitosan (CS-*O*-PEG-*CONH*-TAT), (e) TAT peptide. The chemical shift at δ 7.78 belongs to the aromatic protons of the phthaloyl moiety, which is present in the spectra (a), (b) and (c) but disappeared after deprotection as observed in spectra (d). The multiple peaks of oxymethyl groups in PEG at δ 3.3–3.7 cover the signals of the pyranose ring of chitosan in the spectra of (b), (c) and (d). The weak and broad peak at δ 4.3–4.5 were from the protons of $-\text{NH}-\text{CH}(\text{CH}_2)-\text{CO}-$ in the TAT peptide (e), whose presence is also observed in spectra (d). The peak at δ 2.7–2.8 is from the protons of $-\text{CH}_2-\text{NH}-\text{NH}-\text{NH}_2$ in arginine and the weak and multiple peaks at δ 1.3–1.7 are from the $-\text{CH}_2-\text{CH}_2-\text{CH}_2-\text{NH}-\text{NH}-\text{NH}_2$ in arginine are observed in spectra (c) and (d), which confirms the presence of TAT, when compared to spectra (e). The multiple peaks at δ 7.0–8.0 belong to the amines in the TAT peptide sequence (e) and the similar peaks are observed in the final derivatized polymer (d).

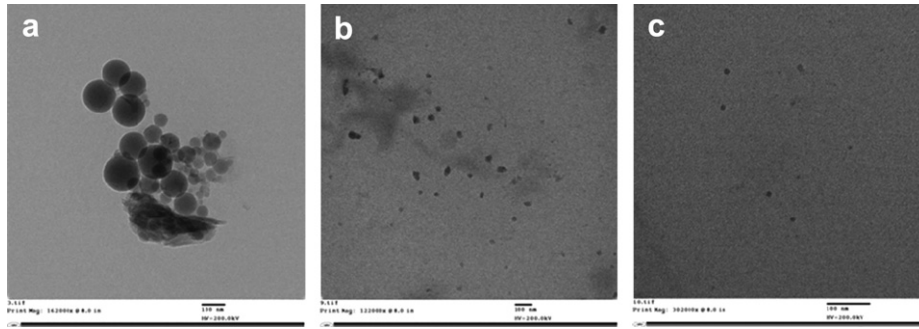


Fig. 6. Nanoparticle characterization using TEM: (a) Empty TAT tagged PEGylated chitosan nanoparticles; magnification: 162,000 \times (b) Unmodified chitosan-siRNA nanoparticles; magnification: 122,000 \times ; (c) Chitosan-PEG-TAT-siRNA nanoparticles; magnification: 302,000 \times .

(b) and (c) represent nanoparticles formed with unmodified chitosan complexing siRNA and Chitosan-PEG-peptide polymer complexing siRNA respectively. On encapsulating siRNA, the nanoparticles obtained from chitosan-PEG-peptide polymer were smaller than 5 nm and appeared more spherical and monodispersed, as compared to the particles obtained by unmodified chitosan polymer, which were 20–50 nm and non-spherical.

3.8. Cell study

Fig. 7b and d represent 100% transfection efficiency, achieved with both unmodified chitosan nanoparticles and chitosan-PEG-TAT nanoparticles encapsulating siGLO-red. The nanoparticle treatment was replaced by fresh media after 4 h and the fluorescence at a wavelength of 660 nm was observed after 24 h. The cells' morphology as observed under bright-field revealed that the cells treated with unmodified chitosan nanoparticles (Fig. 7a) were

stressed as compared to the cells treated with nanoparticles formed from chitosan-PEG-TAT polymer (Fig. 7c). The quantitative and comparative analysis of the cellular toxicity of the two nanoparticle formulations were also tested using the MTS assay, which proved that unmodified chitosan nanoparticles were highly toxic on cells as compared to modified chitosan-PEG-TAT nanoparticles ($p = 0.00004$) (Fig. 8). The modified chitosan-PEG-TAT nanoparticles did not induce any significant toxicity when compared to the untreated cells ($p = 0.507$).

3.9. Protein extraction and western blot

Neuro2a cells, over-expressing Ataxin-1 protein, in-vitro were established prior to the treatment with nanoparticles. Suppression of ataxin protein by Atxn-siRNA delivered through chitosan-PEG-TAT nanoparticles is depicted in Fig. 9. The nanoparticle treatment was replaced after 4 h with complete fresh media and the

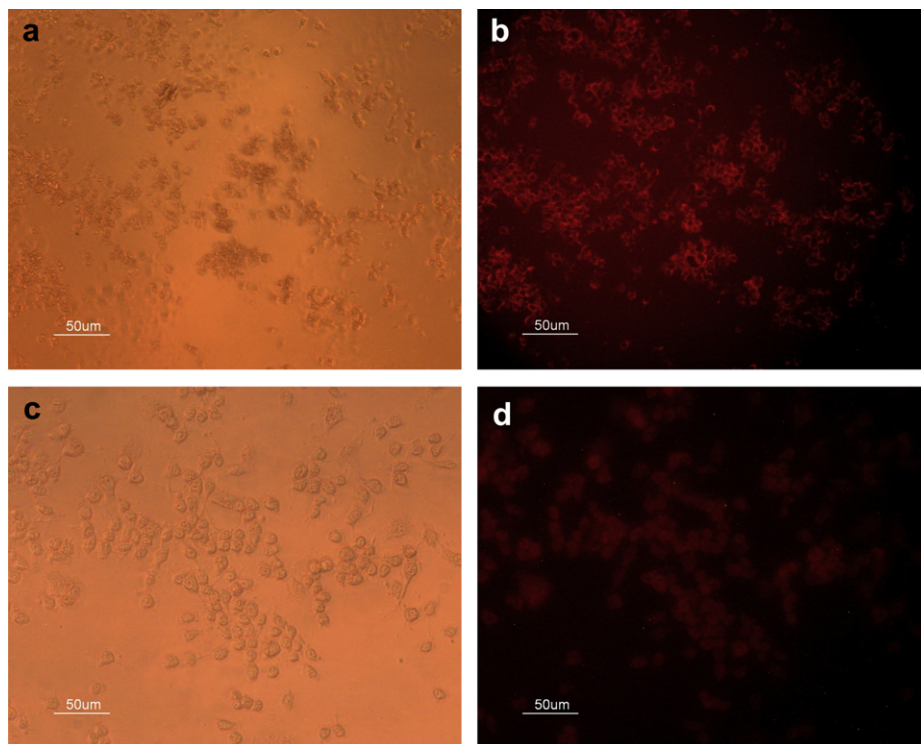


Fig. 7. Cell transfection study on mouse neuroblastoma cells (Neuro2a) transfected with nanoparticles formulation carrying non-targeting Cy-5 labeled scrambled siRNA: (a, b) Cells transfected with unmodified chitosan nanoparticles; (c, d) Cell transfection with modified chitosan-PEG-TAT nanoparticles. It is observed that modified chitosan nanoparticles (d) were equally efficient in transfecting siGLO as unmodified chitosan nanoparticles (b). When compared to the bright field images of the cells, it is clear that the modified nanoparticles (c) pose less cytotoxicity as compared to the unmodified ones (a).

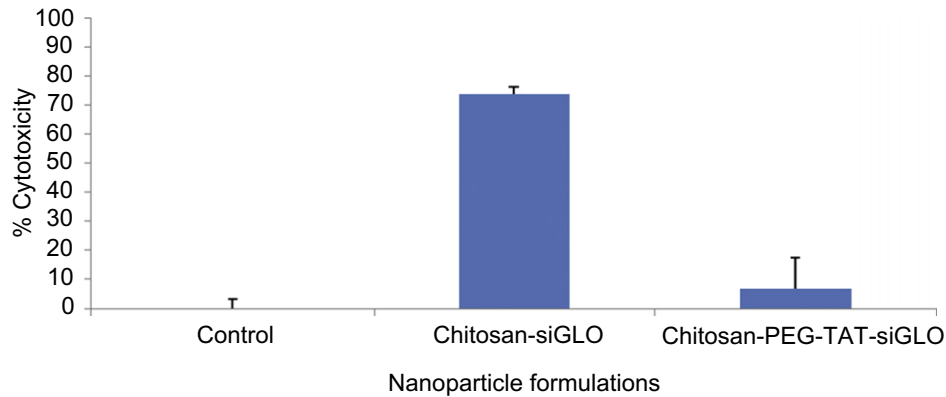


Fig. 8. Cytotoxicity study on mouse neuroblastoma cells (Neuro2a) with various treatments using MTS assay: Unmodified chitosan nanoparticles were highly toxic on cells as compared to modified chitosan-PEG-TAT nanoparticles ($p = 0.00004$). The modified chitosan-PEG-TAT nanoparticles did not induce any significant toxicity when compared to the untreated cells ($p = 0.507$). Data is presented as mean \pm standard deviation, $n = 3$.

cells were harvested after 24 and 48 h for protein quantification. Sample A was treated with nanoparticles with siRNA, Sample B had nanoparticles with Atx-siRNA and sample C had nanoparticles with scrambled siRNA, siGLO. The silencing was observed after 48 h in sample B. This confirmed our hypothesis that nanoparticles prepared using the proposed synthetic scheme successfully and efficiently transfected functional siRNA causing suppression of ataxin protein in neuronal cells in-vitro.

4. Discussion

The blood–brain barrier (BBB) is characterized by tight junctions between cerebral endothelial cells that guard the selective diffusion of blood borne compounds from entering the brain [25]. However, small lipophilic molecules such as glucose, amino acids and gases diffuse freely across the plasma membrane either via carrier-mediated or receptor-mediated mechanisms [26]. Thus, importing drugs or therapeutic molecules across the BBB is a major challenge for the treatment of neurodegenerative diseases. Most of the non-viral nanoparticles widely being accepted as an alternative approach to gene delivery are developed from polyethyleneimine (PEI) [27], chitosan [28], cyclodextrin polycations [29], poly-L Lysine [30] and polyamidoamines [31] to deliver siRNA for on-target gene silencing. The characteristic features encompassing the non-viral nanoparticles for an effective gene delivery system are: 1) the polymeric material should be inert and have low integration with the physiological system, 2) it should handle more payload, 3) can be modified with appropriate ligands for specific cell targeting, 4) be administered repeatedly without fretting about delivery induced toxicity or immunogenicity, 5) should ideally be ≤ 100 nm in size

with a positive surface charge, 6) should be able to overcome anatomical, biophysical and physiological barriers, 7) should be able to safe-guard the payload against degradative enzymes before reaching the targeted site and 8) be able to be administered non-invasively. As per these key features of non-viral nanoparticles, having a small size range is one of the key factors to cross the BBB. Lipid nanoparticles have been used for drug delivery, targeting the brain [32]; however, such formulations lack active targeting to the tissue of interest. Partridge has explained the use of monoclonal antibody as a targeting moiety on a non-viral liposome nanoparticle targeting the brain [33]. Various other BBB targeting antibodies have been detailed by Shusta et al. [34]. However, the high molecular weight of antibodies makes the overall size of the nanoparticles big, which acts as a hindrance to achieve optimal bio-distribution at the targeted site. In view of size, specific peptides, which have much smaller molecular weight as compared to antibodies have also been utilized as targeting ligands for brain delivery [35].

Chitosan is a cationic polymer, whose use has been widely explored in biomedical fields for its biological activities and neuro-protective properties, such as suppression of beta amyloid formation, acetyl cholinesterase inhibitory activity, anti-neuroinflammatory and anti-apoptotic activities [36]. A recent study demonstrates the use and characterization of chitosan nanoparticles loaded with dopamine for future application towards Parkinson's disease [37]. Another study demonstrated the use of chitosan nanoparticles for targeted peptide delivery, such as caspase inhibitor Z-DEVD-FMK or a fibroblast growth factor to the brain [38]. In this study we used chitosan as a parent polymer to develop nanoparticles, surface grafted with PEG and a cell-penetrating peptide, TAT. Chitosan derives its cationic property from the amine groups present at the C6

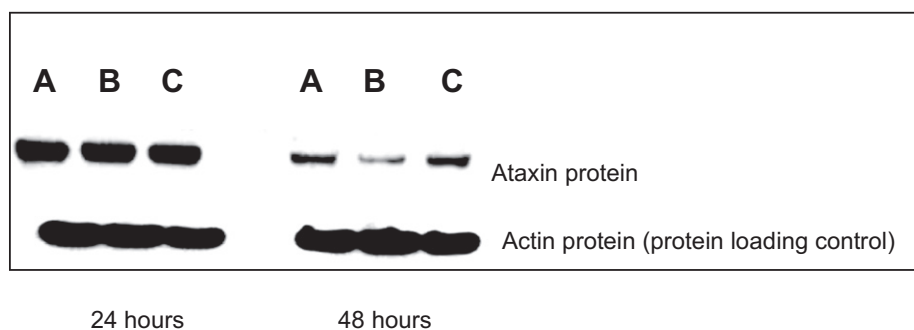


Fig. 9. Western blot analysis of ataxin protein performed after 24 and 48 h: Sample A and C are positive controls with nanoparticles containing no siRNA and scrambled siRNA (siGLO) respectively. Sample B contains nanoparticles with Atxn-siRNA. Silencing is observed after 48 h in sample B. Actin is used as a protein loading control.

position of its pyranose ring. These amine groups are responsible for its solubility only in mild acidic conditions. Though, solubility of chitosan is a major challenge faced when utilizing it for biological applications, it can be controlled by specifically modifying/protecting the primary amine groups thereby making it soluble in solvents like DMSO, DMF, Pyridine, THF etc. [39]. In our study, we protected the amine groups of chitosan by using phthalic anhydride. This property enables it to take part in further chemical reactions. Most of the chitosan derivatives are derived from the chemical modification of NH_2 groups [40]. However, in this study, to form a nanoparticle formulation complexing siRNA, we have employed the use of monomethoxy PEG, a hydrophilic polymer, which was conjugated to the C6 hydroxyl groups of chitosan polymer. This protocol was adapted from Jian Du et al. [23] with a modification of using phthaloyl chitosan. In their procedure they achieved N-substitution as well as O-substitution of chitosan with PEG as their objective did not require protecting primary amines of chitosan, whereas we attempted to obtain chemoselective O-substitution of PEG onto the chitosan [41]. This chemoselective conjugation helps preserve the inherent nature of the cationic polymer by protecting its amine groups with phthalic anhydride [42]. In our previous study, we developed PEGylated chitosan nanoparticles via chemoselective O-substitution of PEG onto chitosan using NHS as a catalyst [42]. However, the current method does not incorporate the use of NHS in the synthesis because the current method yields a higher rate of PEGylated chitosan polymer than the previous method. The conjugation of a hydrophilic polymer (PEG) helps reduce the steric-hindrance and cyto-toxicity of formed nanoparticles and also acts as a linker to further conjugate a cell-penetrating peptide (TAT), which was incorporated to enhance the cellular uptake profile of nanoparticles.

The polymer characterization in terms of pH, concentration and siRNA loading etc. was previously reported by us for preparing chitosan nanoparticles [43] and therefore we used same optimized conditions for unmodified and modified chitosan-PEG-TAT nanoparticles. The TEM image in Fig. 6 represent the nanoparticles developed before and after complexing siRNA with TAT tagged chitosan-PEG-TAT, Fig. 6a and c respectively. The reduction in size from 100 to approximately 5 nm after complexing siRNA is because of the negatively charged siRNA, which forms tight complexes with cationic polymer via electrostatic interactions. Also during the polymer synthesis, the use of hydrazine monohydrate involved in the last step of the synthesis to deprotect the chitosan amine groups, is thought to break the backbone of chitosan chain, yielding smaller chain lengths, allowing us to achieve a smaller particle size. Fig. 6b represents nanoparticles formed with unmodified chitosan complexing siRNA. The particles obtained were in the range of 50–80 nm in size, were polydispersed and non-spherical in shape. The spherical shape of the nanoparticles in Fig. 6a and c is attributed to the PEG in the formulation, which is hydrophilic in nature.

As observed in Fig. 7, the modified chitosan-PEG-TAT nanoparticles were as efficient in delivering siGLO (scrambled siRNA) to neuronal cells (Neuro2a) (Fig. 7d) as the unmodified chitosan nanoparticles (Fig. 7b). However, the morphology of the cells in bright-field for modified chitosan-PEG-TAT nanoparticles looked much healthier than unmodified chitosan nanoparticles. This effect was further evaluated with MTS, a cytotoxicity assay in Fig. 8, which clearly indicates that the modified chitosan-PEG and chitosan-PEG-TAT nanoparticles were significantly less toxic to the cells than the unmodified chitosan nanoparticles. The use of chitosan polymer, TPP and siGLO alone were used as controls to indicate that the major toxic effect in the unmodified chitosan nanoparticles came from chitosan polymer alone, which is again attributed to free amine groups on chitosan. Though it is known that chitosan is a non-toxic polymer however excess of positive charge on its

surface can break the integrity of the cell membrane, causing cell death. Thus, we attempted to modify chitosan's surface before forming nanoparticles in order to reduce the toxic effects, without compromising its transfection efficiency. Lastly, to determine whether these modified chitosan-PEG-TAT nanoparticles can deliver a functional siRNA, we attempted to prove that in an established in-vitro model of SCA1, wherein the neuronal cells were transfected with ataxin-1 plasmid using lipofectamine to over-express ataxin-1 protein. After 24 h of expression the cells were transfected with ataxin-1 siRNA delivered through modified chitosan-PEG-TAT nanoparticles. The results indicate ataxin1 protein suppression after 48 h, as analyzed by western blot. Thus, this study confirms that we successfully achieved 100% transfection of siRNA in neuronal cells with minimal toxicity, with ability to silence a diseased gene causing a therapeutic effect.

5. Conclusion

The article details a scheme for tagging TAT peptide onto the PEGylated chitosan polymer and the formation of nanoparticles capable of delivering siRNA to neuronal cells. The chitosan polymer formulations were characterized using FTIR and NMR at each step of synthesis. The morphological studies were performed using TEM, which revealed nanoparticles as small as 5 nm in size. The chitosan-PEG-TAT nanoparticles were shown to deliver siRNA to neuronal cells with minimal toxicity. They also had an important therapeutic effect in an in-vitro model of SCA. Thus, these nanoparticles hold great promise for biomedical engineering applications, specifically for the delivery of therapeutic molecules targeting neurodegenerative diseases. However, it may be noted that the synthesis and development of these nanoparticles is not limited to one application but represents a platform technology in which the nanoparticles can be custom-made to target any disease application by simply replacing the targeting moiety on the surface of the nanoparticles and the therapeutic payload.

Acknowledgment

We gratefully acknowledge the assistance Natural Sciences and Engineering Research Council of Canada (NSERC) to Dr. S. Prakash, the support of FRSQ doctoral scholarship to M. Malhotra and an NSERC Alexander Graham Bell Graduate doctoral scholarship to C. Tomaro-Duchesneau. We also acknowledge the support of colleagues Rishi Sharma and Anjali Sharma, Department of Chemistry, Otto Maas chemistry Building, McGill University and Ambika Srinivasan, Montreal Neurological Institute, McGill University for their expert opinion to M. Malhotra. We would also like to thank Dr. Zoghbi Huda (Baylor college of medicine, Houston, TX, USA) for providing [pGFP-ataxin (Q82)] was a kind gift, Dr. Jing Hu for synthesizing peptide sequences at Sheldon Biotechnology, McGill University. Dr. Tara Sprules, NMR Facility Manager of Quebec/Eastern Canada NMR Centre for processing our NMR samples, Mr. Petr Fiurasek, Centre for self-assembled Chemical Structures (CSACS) for the FTIR facility, Mr. Xu Dong Liu for processing TEM images at (FEMR) Facility of Electron Microscopy Research at McGill University.

References

- [1] Bettencourt C, Lima M. Machado-joseph disease: from first descriptions to new perspectives. *Orphanet J Rare Dis* 2011;6:35.
- [2] Prakash S, Malhotra M. Recent advancements in targeted delivery of therapeutic molecules in neurodegenerative disease—spinocerebellar ataxia—opportunities and challenges. *Drug Target Insights* 2008;3:99–117.
- [3] Di Prospero NA, Baker A, Jeffries N, Fischbeck KH. Neurological effects of high-dose idebenone in patients with Friedreich's ataxia: a randomized, placebo-controlled trial. *Lancet Neurol* 2007;6:878–86.

- [4] Xia H, Mao Q, Eliason SL, Harper SQ, Martins IH, Orr HT, et al. RNAi suppresses polyglutamine-induced neurodegeneration in a model of spinocerebellar ataxia. *Nat Med* 2004;10:816–20.
- [5] Dorn G, Patel S, Wotherspoon G, Hemmings-Mieszczyk M, Barclay J, Natt FJ, et al. siRNA relieves chronic neuropathic pain. *Nucleic Acids Res* 2004;32:e49.
- [6] Takei Y, Kadomatsu K, Yuzawa Y, Matsuo S, Muramatsu T. A small interfering RNA targeting vascular endothelial growth factor as cancer therapeutics. *Cancer Res* 2004;64:3365–70.
- [7] Zhang Y, Zhang YF, Bryant J, Charles A, Boado RJ, Pardridge WM. Intravenous RNA interference gene therapy targeting the human epidermal growth factor receptor prolongs survival in intracranial brain cancer. *Clin Cancer Res* 2004;10:3667–77.
- [8] Bhoomik A, Jones N, Ronai Z. Transcriptional switch by activating transcription factor 2-derived peptide sensitizes melanoma cells to apoptosis and inhibits their tumorigenicity. *PNAS* 2004;101:4222–7.
- [9] Pardridge WM. Blood–brain barrier drug targeting: the future of brain drug development. *Mol Interv* 2003;51:90–105.
- [10] Lu PY, Xie F, Woodle MC. In vivo application of RNA interference: from functional genomics to therapeutics. *Adv Genet* 2005;54:117–42.
- [11] Arai K, Kineemaki T, Fujita T. Toxicity of chitosan. *Bull Tokai Reg Fish Res Lab* 1968;56:89–94.
- [12] Yamamoto H, Amaike M. Biodegradation of cross-linked chitosan gels by microorganisms. *Macromolecules* 1997;30:3936–7.
- [13] Risbud MV, Bhande RR. Polyacrylamide-chitosan hydrogels: in vitro biocompatibility and sustained antibiotic release studies. *Drug Deliv* 2000;7:69–75.
- [14] Working PK, Newman MS, Johnson J, Cornacoff JB. Safety of poly(ethylene glycol) and poly(ethylene glycol) derivatives. In: Harris JM, Zalipsky S, editors. *Polyethylene glycol chemistry and biological applications*. Washington DC: American Chemical Society; 1997. p. 45.
- [15] Sugimoto M, Morimoto M, Sashiwa H, Saimoto H, Shigemasa Y. Preparation and characterization of water-soluble chitin and chitosan derivatives. *Carbohydr Polym* 1998;36:49–59.
- [16] Ouchi T, Nishizawa H, Ohya Y. Aggregation phenomenon of peg-grafted chitosan in aqueous solution. *Polymer* 1998;39:5171–5.
- [17] Lebouc F, Dez I, Desbrieres J, Pictou L, Madec PJ. Different ways for grafting ester derivatives of poly(ethylene glycol) onto chitosan: related characteristics and potential properties. *Polymer* 2005;46:639–51.
- [18] Kircheis R, Kichler A, Wallner G, Kurska M, Ogris M, Felzmann T, et al. Coupling of cell-binding ligands to polyethyleneimine for targeted gene delivery. *Gen Ther* 1997;4:409–18.
- [19] Moore NM, Sheppard CL, Sakiyama-Elbert SE. Characterization of a multifunctional peg-based gene delivery system containing nuclear localization signals and endosomal escape peptides. *Acta Biomater* 2009;5:854–64.
- [20] Torchilin VP, Rammohan R, Weissig V, Levchenko TS. TAT peptide on the surface of liposomes affords their efficient intracellular delivery even at low temperature and in the presence of metabolic inhibitors. *Proc Natl Acad Sci USA* 2001;98:8786–91.
- [21] Tseng YL, Liu JJ, Hong RL. Translocation of liposomes into cancer cells by cell-penetrating peptides penetratin and TAT: a kinetic and efficacy study. *Mol Pharmacol* 2002;62:864–72.
- [22] Kurita K, Ikeda H, Yoshida Y, Shimojoh M, Harata M. Chemoselective protection of amino groups of chitosan by controlled phthaloylation: facile preparation of a precursor useful for chemical modifications. *Biomacromolecules* 2002;3:1–4.
- [23] Du Jian, Hsieh You-Lo. Pegylation of chitosan for improved solubility and fiber formation via electrospinning. *Cellulose* 2007;14:543–52.
- [24] Lin WJ, Chen MH. Synthesis of multifunctional chitosan with galactose as a targeting ligand for glycoprotein receptor. *Carbohydr Polym* 2007;67:474–80.
- [25] Rubin LL, Staddon JM. The cell biology of the blood–brain barrier. *Annu Rev Neurosci* 1999;22:11–28.
- [26] Pardridge WM. In: *Peptide drug delivery to the brain*. New York: Raven Press; 1991. p. 1–357.
- [27] Schifferers RM, Ansari A, Xu J, Zhou Q, Tang Q, Storm G, et al. Cancer siRNA therapy by tumor selective delivery with ligand-targeted sterically stabilized nanoparticle. *Nucleic Acids Res* 2004;32:e149.
- [28] Katas H, Alpar HO. Development and characterisation of chitosan nanoparticles for siRNA delivery. *J Control Release* 2006;115:216–25.
- [29] Bartlett DW, Su H, Hildebrandt IJ, Weber WA, Davis ME. Impact of tumor-specific targeting on the biodistribution and efficacy of siRNA nanoparticles measured by multimodality in vivo imaging. *Proc Natl Acad Sci USA* 2007;104:15549–54.
- [30] Inoue Y, Kurihara R, Tsuchida A, Hasegawa M, Nagashima T, Mori T, et al. Efficient delivery of siRNA using dendritic poly(l-lysine) for loss-of-function analysis. *J Control Release* 2008;126:59–66.
- [31] Patil ML, Zhang M, Betigeri S, Taratula O, He H, Minko T. Surface-modified and internally cationic polyamidoamine dendrimers for efficient siRNA delivery. *Bioconjug Chem* 2008;19:1396–403.
- [32] Wissing SA, Kayser O, Müller RH. Solid lipid nanoparticles for parenteral drug delivery. *Adv Drug Deliv Rev* 2004;56:1257–72.
- [33] Xia CF, Zhang Y, Zhang Y, Boado RJ, Pardridge WM. Intravenous siRNA of brain cancer with receptor targeting and avidin–biotin technology. *Pharm Res* 2007;24:2309–16.
- [34] Jones AR, Shusta EV. Antibodies and the blood–brain barrier. In: *Therapeutic monoclonal antibodies: from bench to clinic*. John Wiley & Sons, Inc. p. 483–502.
- [35] Sharma V, Piwnicka-Worms D. Blood–brain barrier permeation peptides. *US Patent No. US7,803,351 B2*, 2010.
- [36] Pangestuti R, Kim SK. Neuroprotective properties of chitosan and its derivatives. *Mar Drugs* 2010;8:2117–28.
- [37] Giglio E, Trapani A, Cafagna D, Sabbatini L, Cometa S. Dopamine-loaded chitosan nanoparticles: formulation and analytical characterization. *Anal Bioanal Chem* 2011;400:1997–2002.
- [38] Caban S, Capan Y, Couvreur P, Dalkara T. Preparation and characterization of biocompatible chitosan nanoparticles for targeted brain delivery of peptides. *Methods Mol Biol* 2012;846:321–2.
- [39] Yoksan R, Matsusaki M, Akashi M, Chirachanchai S. Controlled hydrophobic/hydrophilic chitosan: colloidal phenomena and nanosphere formation. *Colloid Polym Sci* 2004;282:337–42.
- [40] Kumar MNVR, Muzzarelli RAA, Muzzarelli C, Sashiwa H, Domb AJ. Chitosan chemistry and pharmaceutical perspectives. *Chem Rev* 2004;104:6017–84.
- [41] Gorochoveva N, Makuška R. Synthesis and study of water-soluble chitosan–O–poly(ethylene glycol) graft copolymers. *Eur Polym J* 2004;40:685–91.
- [42] Malhotra M, Lane C, Tomaro-Duchesneau C, Saha S, Prakash S. A novel method for synthesizing pegylated chitosan nanoparticles: strategy, preparation and in-vitro analysis. *Int J Nanomedicine* 2011;6:485–94.
- [43] Malhotra M, Kulamarva A, Sebak S, Paul A, Bathena J, Mirzaei M, et al. Ultrafine chitosan nanoparticles as an efficient nucleic acid delivery system targeting neuronal cells. *Drug Dev Ind Pharm* 2009;35:719–26.